

Implementation and Validation of an Advanced Hypoplastic Model for Granular Material Behavior

Montaser Bakroon¹, Reza Daryaei¹, Daniel Aubram¹, Frank Rackwitz¹

¹Chair of Soil Mechanics and Geotechnical Engineering, Technische Universität Berlin, Berlin, Germany

Abstract

*Problems in soil mechanics and geotechnical engineering are often characterized by large deformations and complex material behavior. For example, the mechanical behavior of granular materials like sand is highly nonlinear due to the presence of an evolving internal structure formed by the grains. The strength and stiffness is generally a function of the stress and density state and the loading history. While LS-DYNA® has proved to be among the most robust hydrocodes for modelling large deformations and dynamic problems, it currently does not provide material models capturing granular material behavior over a wide range of stress and density states under monotonic and cyclic loads with only one set of parameters for a specific granular material and incorporating state parameters such as void ratio. Therefore, an advanced soil mechanical constitutive equation based on the hypoplasticity framework has been implemented in LS-DYNA using the UMAT interface in conjunction with the *USER_DEFINED_MATERIAL_MODEL keyword. The implemented hypoplastic model defines evolution equations for the effective stress, void ratio, and the so-called intergranular strain tensor suitable for simulating cyclic loading effects. Previously, the model has been successfully implemented in other hydrocodes. However, in comparison to other hydrocodes, LS-DYNA employs more advanced element technology, such as the Multi-Material Arbitrary Lagrangian Eulerian (MMALE) formulation, to simulate large deformation problems. The motivation of this study was to combine the hypoplastic material model with MMALE to study more realistically problems in soil mechanics and geotechnical engineering. The implementation is validated by comparing to results of oedometer and triaxial laboratory tests. It is shown that the UMAT is able to simulate soil behavior under cyclic loading and undrained conditions. The combination of the UMAT with MMALE is evaluated using the example of a sand column collapse. The numerical results are in good agreement with experimental test results and can be seen as a promising starting point for further applications.*

Introduction

Capturing the complex nonlinear mechanical behavior of granular materials, such as sandy soils, is one of the key aspects in geotechnical analysis and design. The accuracy of numerical simulations is in a large part influenced by the choice of the material model. Moreover, geotechnical problems are often characterized by large deformations, hence there is an increasing interest for combining advanced soil material models with suitable and robust element formulations in order to reach a convergent and reliable solution.

Conventional approaches to constitutive modeling of soils are based on elastoplasticity. By using this theory, a yield surface and plastic surface must be defined, which means that in a specific range of admissible states the material behaves purely elastic. In an elastic state, the induced strain is reversible by unloading, which is generally not the case for granular soils. The class of constitutive equations based on the so-called “hypoplasticity” concept, on the other hand, does not distinguish between elastic and plastic states and have been proven more accurate in simulating the complex behavior of granular materials under cyclic loading and over a wide range of stress and density states with only one set of parameters for a specific granular material and incorporating state parameters such as void ratio [1–4]. Besides, by removing extra definitions regarding yield and plastic surface, such models are easier to implement [5].

The first hypoplastic constitutive model was proposed by Kolymbas in 1977 [6]. Since then, various extensions have been developed. One of the most comprehensive hypoplastic constitutive equations has been developed by Gudehus [7] and calibrated by Bauer [8]. Later, von Wolffersdorff [9] improved the mathematical formulation of this model. Finally, Niemunis and Herle [10] resolved the associated problems in strain accumulation in cyclic loading by defining a new state variable called intergranular strain. The hypoplastic model with intergranular strain is also used in this study. This material model is extensively used in numerical simulations of geotechnical problems, and different implementations in various finite element codes are available [11]. The

research work presented in this paper is concerned with the implementation of the hypoplastic model into LS-DYNA and the application of advanced element technology such as MMALE to geotechnical problems.

The ALE method developed by Hirt et al. [12] has been extensively used to address mesh distortion issues attributed to classical FEM approaches. The general strategy is to perform three sub-steps which are sequentially arranged as a Lagrangian step, a rezone step, and a remap step. In the Lagrangian step, the mesh deforms as the material deforms. The rezone step generates a new computational grid to diminish the distortion associated with the Lagrangian step. The updated mesh is not necessarily identical to the original mesh. If the new computation grid is identical to the original mesh, this method is called a Eulerian method. Finally, the remap step transports the material from the old mesh to the new arbitrary mesh.

The ALE is generally categorized as single/simplified ALE (SALE) and multi-material ALE (MMALE). In SALE the rezoning and remapping applies inside material boundaries. By using SALE, the problems associated with classical Lagrangian is to some extent solved for specific problems and provide better results [13]. The material boundaries still impose limitations in mesh improvement, i.e. by extremely large deformation the distortion is still significant. On the other hand, MMALE introduces additional non-filled mesh elements. The material boundaries (or interfaces) can therefore flow through the mesh, which imposes no restrictions concerning the magnitude of material deformation. The interface between multiple materials are subsequently reconstructed and tracked. *Fig. 1* illustrates the MMALE sub-steps as well as interface reconstruction in one MMALE calculation cycle. Details can be found in [14,15].

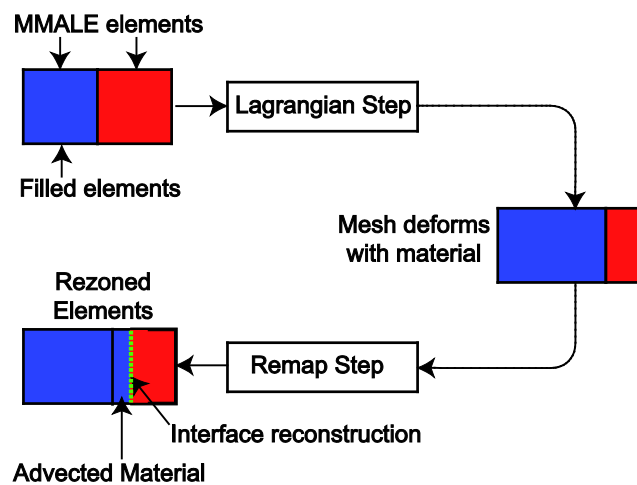


Fig. 1. Schematic diagram of MMALE sub-steps in one calculation cycle for one dimensional flow [2].

Several studies have been done using advanced element formulations with hypoplastic material models. Dijkstra et al. [4] modelled pile installation in saturated soil using ALE method. In his study, an elastic pile is fixed and the soil flows around the pile. The computational model handled the large soil deformations induced by pile installation and provided comparable results. Qiu et al. [1] used a so-called Coupled Eulerian-Lagrangian (CEL) method and the hypoplastic material model to simulate displacement of a strip footing, pile installation, and ship grounding; the CEL method can be considered as a variant of an MMALE method where the solution is remapped onto the original, i.e. Eulerian mesh. The results were satisfactory for such problems. Another study was conducted by Pucker and Grabe [3] to study the affecting parameters on the rotary pile installation. The numerical results were used to explain the soil state after drilling which was measured at the site.

In this study, the implementation of the hypoplastic material model into LS-DYNA is verified and validated using basic benchmarks, oedometer and triaxial element tests. Subsequently, a real-size experiment is simulated using the implemented material model in conjunction with the available MMALE technology.

The structure of this work is as follows. First, the theoretical background of the hypoplastic material model is presented. Then, the implementation is explained and results of the example applications are discussed in detail. The paper closes with some concluding remarks.

Hypoplastic model for granular material

The hypoplastic material model used in this study is the one developed by von Wolffersdorff [9] which is considered as the enhanced version of the constitutive model introduced by Gudehus [7] and Bauer [8]. A further modification was applied by Niemunis and Herle [10] which will be described later in this section. The hypoplastic concept employs a closed form expression relating the co-rotational Jaumann rate of effective stress of the grain skeleton to the stretching, with no distinction between elastic and plastic deformation. Some of the main assumptions are defined as follows [10]:

1. The mechanical behavior of the granular material is completely determined by the effective stress, \mathbf{T} , and void ratio, e .
2. Grains (soil particles) are assumed rigid and permanent during the whole process (i.e. no crushing compression or abrasion of grains). Therefore, the deformation is attributed to change in void ratio or rearrangement of grain contacts only.
3. Loading rate effects are not considered.
4. Homogeneity of the soil is maintained at homogenous boundary conditions (e.g. no shear localization).
5. The void ratio, i.e. the ratio of the pore volume and solid volume, is constrained by three limiting void ratios. Two upper and lower void ratios, e_i and e_d corresponding to minimum and maximum density, respectively. The third limiting parameter is the void ratio at critical state, e_c .
6. A granular hardness parameter, h_s , is defined to adapt the limiting void ratio parameters based on the current mean pressure.

Hypoplasticity predicts the nonlinear and inelastic behavior of granular materials quite well. The constitutive model can detect some of the main interesting soil properties like dilatancy, that is, the increase void ratio due to shear loading. Accordingly, the dependency on the void ratio of the soil allows for realistic simulation of compaction processes. The novelty of hypoplastic constitutive model is that the soil behavior under loading and unloading condition is defined by a single incrementally nonlinear equation, unlike elastoplastic material models. This is done by considering the strain path and the current void ratio. The hypoplastic constitutive equation takes the form [16]:

$$\dot{\mathbf{T}} = \mathcal{L} : \mathbf{D} + \mathbf{N} \|\mathbf{D}\| \quad (1)$$

where $\dot{\mathbf{T}}$ denotes the co-rotational Jaumann stress rate, \mathbf{D} is the strain/stretching rate tensor, $\mathcal{L}(\mathbf{T}, e)$ is a fourth-order tensor associated with the linear part of the behavior and $\mathbf{N}(\mathbf{T}, e)$ is a second-order tensor related to the nonlinear part of the behavior. The accuracy and performance of hypoplasticity is mainly dependent on $\mathcal{L}(\mathbf{T}, e)$ and $\mathbf{N}(\mathbf{T}, e)$ which are defined by Eq. (2) and (3):

$$\mathcal{L} = \frac{f_b f_e}{\hat{\mathbf{T}} : \hat{\mathbf{T}}} a^2 \left(\left(\frac{F}{a} \right)^2 \mathbf{I} + \hat{\mathbf{T}} : \hat{\mathbf{T}} \right) \quad (2)$$

$$\mathbf{N} = \frac{f_d f_b f_e}{\hat{\mathbf{T}} : \hat{\mathbf{T}}} a^2 \left(\frac{F}{a} \right) (\hat{\mathbf{T}} + \hat{\mathbf{T}}^*) \quad (3)$$

where

$$a = \frac{\sqrt{3}(3 - \sin \phi_c)}{2\sqrt{2}\sin \phi_c} \quad (4)$$

$$f_b = \left(\frac{e_{i0}}{e_{c0}}\right)^\beta \frac{h_s}{n} \frac{1 + e_i}{e_i} \left(\frac{-tr\mathbf{T}}{h_s}\right)^{1-n} \times \left[3 + a^2 - a\sqrt{3} \left(\frac{e_{i0} - e_{d0}}{e_{c0} - e_{d0}}\right)^\alpha\right]^{-1} \quad (5)$$

$$f_d = \left(\frac{e - e_d}{e_c - e_d}\right)^\alpha \quad (6)$$

$$f_e = \left(\frac{e_c}{e}\right)^\beta \quad (7)$$

$$F = \sqrt{\frac{1}{8} \tan^2 \psi + \frac{2 - \tan^2 \psi}{2 + \sqrt{2} \tan \psi \cos 3\theta} - \frac{1}{2\sqrt{2}} \tan \psi} \quad (8)$$

$$\tan \psi = \sqrt{3} \|\hat{\mathbf{T}}^*\| \quad (9)$$

$$\cos 3\theta = -\sqrt{6} \frac{tr(\hat{\mathbf{T}}^* \cdot \hat{\mathbf{T}}^* \cdot \hat{\mathbf{T}}^*)}{[\hat{\mathbf{T}}^* : \hat{\mathbf{T}}^*]^{3/2}} \quad (10)$$

$$\hat{\mathbf{T}} = \frac{\mathbf{T}}{tr \mathbf{T}} \quad (11)$$

$$\hat{\mathbf{T}}^* = \hat{\mathbf{T}} - \frac{1}{3} \mathbf{I} \quad (12)$$

$$\frac{e_i}{e_{i0}} = \frac{e_c}{e_{c0}} = \frac{e_d}{e_{d0}} = \exp \left[- \left(\frac{-tr\mathbf{T}}{h_s} \right)^n \right] \quad (13)$$

Where f_b is the barotropy factor and f_e and f_d are the pycnotropy factors. The barotropy factor relates the void ratio to mean pressure while the pycnotropy factors consider densification effects. The definition of other parameters appeared in Eq. (4)-(13) are listed in *Table 1*.

The hypoplastic material model in the form of Eq. (1) accurately predicts granular material behavior under monotonic loads and sufficiently large strains. However, under cyclic loads excessive strain accumulation can be observed. By introducing a so-called intergranular strain tensor together with a refined small strain stiffness formulation, the reference model could be improved [10]. The improved constitutive model is rewritten as:

$$\dot{\mathbf{T}} = \mathcal{M}(\mathbf{T}, e, \delta) : \mathbf{D} \quad (14)$$

Where \mathcal{M} is the fourth order tensor depending on the stress tensor, \mathbf{T} , void ratio, e , and the intergranular strain δ which represents the stiffness that is calculated from both hypoplastic tensors defined by Eq. (2) and (3), $\mathcal{L}(\mathbf{T}, e)$ and $\mathbf{N}(\mathbf{T}, e)$. The difference in this case, is the dependence of \mathcal{M} on two parameters, the normalized intergranular strain value, ρ , and its direction, $\hat{\delta}$, with the strain rate ($\hat{\delta} : \mathbf{D}$). ρ and $\hat{\delta}$ are defined in Eq. (15) and Eq. (16), respectively.

$$\rho \equiv (|\delta|/R) \quad (15)$$

$$\hat{\delta} \equiv \begin{cases} \delta/|\delta| & \text{for } \delta \neq 0 \\ 0 & \text{for } \delta = 0 \end{cases} \quad (16)$$

The general equation determining the stiffness value \mathcal{M} takes the form:

$$\mathcal{M} = [\rho^\chi m_T + (1 - \rho^\chi) m_R] \mathcal{L} + \begin{cases} \rho^\chi (1 - m_T) \mathcal{L} : \hat{\delta} \hat{\delta} + \rho^\chi \mathbf{N} \hat{\delta} & \text{for } \hat{\delta} : \mathbf{D} > 0 \\ \rho^\chi (m_R - m_T) \mathcal{L} : \hat{\delta} \hat{\delta} & \text{for } \hat{\delta} : \mathbf{D} \leq 0 \end{cases} \quad (17)$$

Where χ is a constant used for smoothing the weighting factor ρ^χ , and m_T and m_R are additional constants which account for changes in loading direction upon unloading/reloading.

Table 1 The required parameters of hypoplastic material model with intergranular strain

<i>Hypoplastic model parameters</i>		<i>Intergranular strain parameters</i>	
<i>Constant</i>	<i>Description</i>	<i>Constant</i>	<i>Description</i>
ϕ_c [°]	Critical friction angle	R	Maximum intergranular strain
h_s [MPa]	Granular hardness	m_R	Stiffness multiplication factor
n	Exponent	m_T	Stiffness multiplication factor
e_{d0}	Min. void ratio	χ	Smoothing constant
e_{c0}	Critical void ratio	β_r	Smoothing constant
e_{i0}	Max. void ratio at zero pressure		
α	Exponent		
β	Exponent		

LS-DYNA UMAT interface implementation

The hypoplastic UMAT interface used in this study is based on the coding of Tamagnini and Masin under soilmodel.info project [11]. The current UMAT version which is already implemented in ABAQUS is used for the interface implementation in LS-DYNA was last revised in 2009. Standard fixed format Fortran 77 language code is used to write the UMAT command lines.

LS-DYNA R9.1.0 is used in this study. The Intel Parallel Studio XE 2015 and Visual Studio 2012 are coupled with LS-DYNA for invoking the user-defined material model. To implement a user-defined interface in LS-DYNA, a new executable file should be linked. The object files and multiple source routines required for this step is made available by LSTC for both Windows[®] or Linux platforms. All the software as well as compilation was run on Microsoft Windows platform. The UMAT is added to dyn21.f file in subroutine UMAT43. Subsequently, the executable file (Lsdyna.exe) is generated using the modified dyn21.f file via nmake command in Intel[®] Visual Fortran Compiler. In the finite element model set up with LS-DYNA, the keyword *MAT_USER_DEFINED_MATERIAL_MODELS is used to define the user material parameters. The required parameters for this subroutine are listed in *Table 2*.

Table 2 Required input parameters for Hypoplastic model in *MAT_USER_DEFINED_MATERIAL_MODELS keyword

Parameter	Description	Value
RO	Mass density	Problem-dependent
MT	User material type	43
LMC	Length of material constant array (number of material constants to be input)	16
NHV	Number of history variables to be stored	16
IORTHO	Orthotropic flag	0 (Non-orthotropic)
IBULK	Address of bulk modulus in material constants array	Problem-dependent
IG	Address of shear modulus in material constants array	Problem-dependent
IVECT	Vectorization flag	0 (non-vectorized)

In LS-DYNA, defining bulk and shear modulus as an input is compulsory for every material model, however, the hypoplastic material model does not take an initial value for such parameters as input, since such parameters are calculated internally. Nevertheless, it is possible to calculate the initial bulk modulus with available hypoplastic parameters using Eq. (18).

$$K = \frac{1}{3} \frac{h_s}{n} \left(1 + \frac{1}{e_p} \right) \left(\frac{3p_s}{h_s} \right)^{1-n} \quad (18)$$

Where K is the bulk modulus and e_p is the void ratio at given skeleton pressure p_s [17]. Other parameters were previously shown in *Table 1*.

During the calculation, LS-DYNA calls the corresponding UMAT subroutine based on the used element type (2D plane strain, plane stress, 3D, etc.) for state variable update. The subroutine usually takes the following form:

Subroutine UMAT43 (cm, eps, sig, epsp, hsv, dt1, capa, etype, tt, temper, fail1, crv)

The inputs of subroutine are listed in *Table 3* as well as its description.

Table 3 UMAT interface variables

Input variables for UMAT	Description
sig(6)	stresses in previous time step
eps(6)	strain increments
epsp	effective plastic strain in previous time step
hsv(*) [†]	history variables in previous time step excluding plastic strain
cm(*) [†]	material constants array
dt1	current time step size
tt	current time
temper	current temperature
fail1	flag indicating failure of element
capa	transverse shear correction factor for shell elements
crv(lq1,2,*)	array representation of curves defined in the keyword deck
etype	character string that equals solid, shell, or beam

[†] The * denotes to a user-defined array size. the maximum size of history variable array and material constants array is by default limited to 142 and 48, respectively.

The numbering order for assigning the stress/strain indices in stress/strain array in LS-DYNA UMAT interface follows the method illustrated in *Table 4*.

Table 4 Stress/strain assignment order in LS-DYNA UMAT

Stress direction	Stress array index	Strain direction	Strain array index
σ_{11}	sig(1)	ϵ_{11}	eps(1)
σ_{22}	sig(2)	ϵ_{22}	eps(2)
σ_{33}	sig(3)	ϵ_{33}	eps(3)
σ_{12}	sig(4)	ϵ_{12}	eps(4)
σ_{23}	sig(5)	ϵ_{23}	eps(5)
σ_{31}	sig(6)	ϵ_{31}	eps(6)

UMAT verification and validation

To verify and validate the performance of the UMAT subroutine of the hypoplastic model with intergranular strain, an oedometer test as well a triaxial test were simulated using a single element. These basic tests were also simulated by Niemunis and Herle [10] and von Wolffersdorff [9]. The implemented UMAT has the feature of switching the intergranular strain on and off. This point makes it possible to compare the implemented model with both references.

Oedometer test

An oedometer test is a common geotechnical test where the soil specimen is placed inside a rigid container and loaded vertically. The lateral displacement of the specimen is constrained by the container to simulate one dimensional compression. It is also possible to apply cyclic loading during the test. In this case, the soil particles are rearranged during repeated loading and unloading, leading to an accumulative compaction. Realistic prediction of accumulated compaction by numerical simulation is not an easy task, but the results produced by the hypoplastic model with intergranular strain are reasonable. The schematic figure of the oedometer test as well as its finite element model equivalent is demonstrated in *Figure 2*. The soil used for the simulation is Hochstetten sand whose hypoplastic parameters are summarized in *Table 5*. The initial void ratio of the sand is chosen as $e_0 = 0.695$, and vertical stress is increased monotonically until a maximum value of $\sigma_1 = 1$ MPa is reached. Subsequently, a cyclic load varying between 0.5 MPa and 0.8 MPa is applied.

Table 5 Hypoplastic parameters of Hochstetten sand for Oedometer test [10]

φ_c [°]	h_s [MPa]	n	e_{d0}	e_{c0}	e_{i0}	α	β	m_R	m_T	R	χ	β_r
33	1000	0.25	0.55	0.95	1.05	0.25	1	5.0	2.0	1×10^{-4}	6.0	0.5

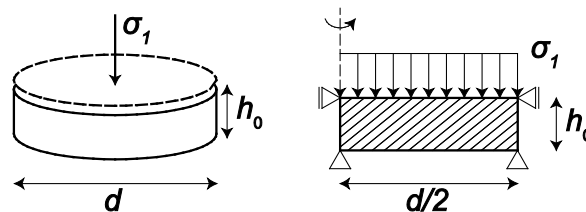


Figure 2 (a) Schematic of the Oedometer test; (b) FE-mesh and boundary conditions

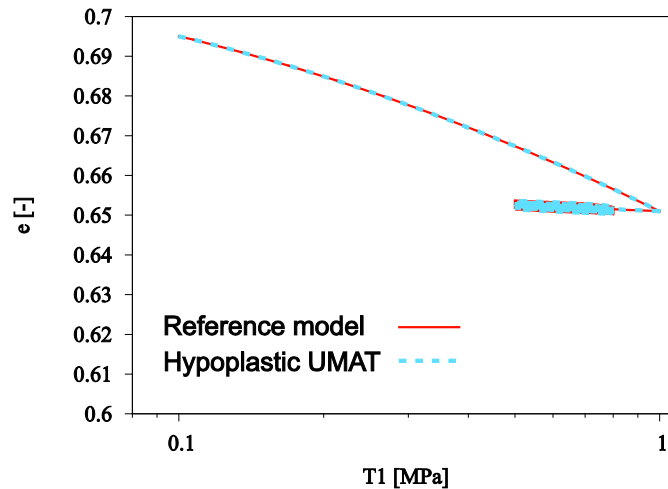


Figure 3 Void ratio vs. vertical stress curve for oedometric compression test using the Hypoplastic UMAT

Figure 3 shows the resulting void ratio vs. vertical stress curve obtained from the compression test. The curve from the implemented UMAT is compared with the one obtained from Niemunis & Herle [10] in Figure 3. It can be observed that the implemented UMAT provides perfectly consistent results according to reference models.

Triaxial test

Another common geotechnical test is the triaxial test, where the soil specimen is placed inside a cylindrical chamber filled with water to simulate confining stress present *in-situ*. The concept is to apply different stresses on vertical and horizontal directions on the soil. Initially, the specimen is subjected to equal pressure in all directions (consolidation stage). Subsequently, the vertical stress is increased to evaluate specimen shear strength. From triaxial test, fundamental soil parameters are obtained such as shear strength parameters. The test can be performed under different drainage and sample preparation conditions. However, the focus of this study is on dry sand. Figure 4 shows the schematic of a triaxial test as well as its numerical model equivalent. The material parameters for triaxial test are listed in Table 6. The only difference between Table 6 and Table 5 is the β factor which is taken here as 1.75. The initial void ratio is taken as $e_0 = 0.695$ with initial isotropic stress $\sigma_1 = \sigma_2 = \sigma_3 = 100$ kPa. and the maximum deviator stress is $\sigma_1 = 300$ kPa. Figure 5 shows that the strain vs. stress curve is in good correlation to the reference model by Niemunis and Herle [10].

Table 6 Hypoplastic parameters of Hochstetten sand for triaxial test [10]

φ_c [°]	h_s [MPa]	n	e_{d0}	e_{c0}	e_{i0}	α	β	m_R	m_T	R	χ	β_r
33	1000	0.25	0.55	0.95	1.05	0.25	1.75	5.0	2.0	1×10^{-4}	6.0	0.5

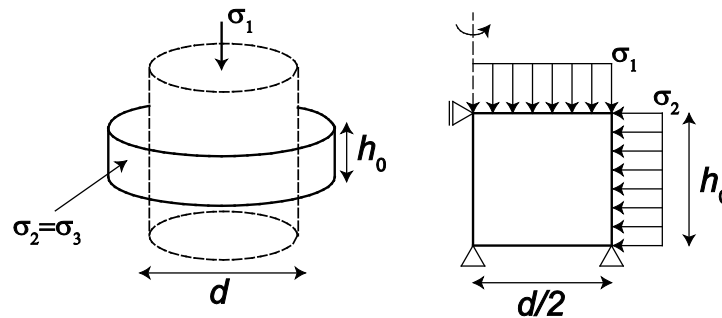


Figure 4 (a) Schematic of the triaxial test (left), FE-mesh and boundary conditions (right)

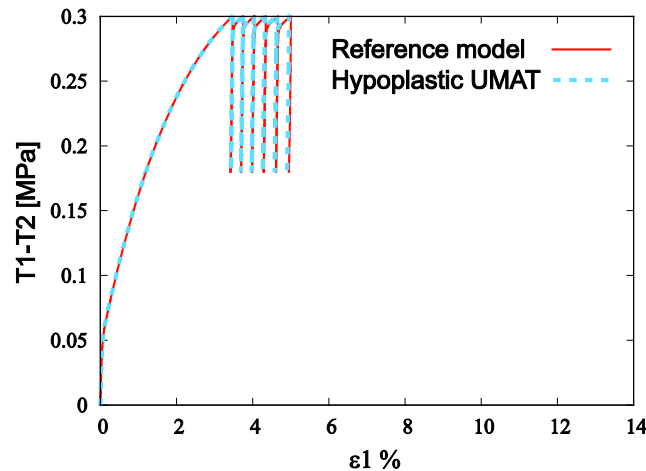


Figure 5 Deviatoric stress vs. axial strain for Triaxial compression test using the Hypoplastic UMAT

Sand column collapse

Collapse of a sand column is an experimental test which has various engineering applications such as determining the angle of repose, debris flow run-out, etc. A column of sand is held in a container and the holding gate is suddenly released allowing the sand to collapse by its own weight. A schematic for this problem is shown in Fig. 6. An experimental study performed by Lube et al. [18] has been chosen as a reference model to analyze the robustness of hypoplastic material subroutine used together with the MMAL capability of LS-DYNA. The experimental results of run-out distance and height of sand column are compared to the obtained numerical values.

In the experiment, the sand column is placed in a rectangular container. Owing to symmetry of the experiment, only half of the column is considered. Then, one side of the rectangular container is lifted abruptly to impose the flow condition. The width of the soil column is $d_i = 0.0905$ m with a height to width aspect ratio of 7. The depth of the test soil in direction normal to flow is 0.2 m. The flowing surface friction is equal to internal friction of the sand.

Unfortunately, the geotechnical parameters of the sand in this experiment are not reported. However, in a different numerical study conducted by Solowski and Sloan [19], the corresponding Mohr-Coulomb material

model parameters for this experiment are reported and listed in *Table 7*. The hypoplastic parameters are estimated to fit the Mohr-Coulomb parameters using numerical simulations of triaxial tests with same conditions described in the previous example. The equivalent hypoplastic properties of the soil are shown in *Table 8*.

Table 7 Anticipated Mohr-Coulomb properties for the sand column test from [19]

Density ρ (kg/m ³)	Friction angle ϕ	Dilatancy angle ψ	Cohesion c (kPa)	Poisson ratio ν	Elastic Modulus E (kPa)
1600	31°	1°	0.001	0.3	840

Table 8 Equivalent Hypoplastic properties of the sand based on the Mohr-Coulomb material model

φ_c [°]	h_s [MPa]	n	e_{d0}	e_{c0}	e_{i0}	e_0	α	β	m_R	m_T	R	χ	β_r
33	10	0.25	0.55	0.95	1.05	0.695	0.25	1.5	5.0	2.0	1×10^{-4}	6.0	0.5

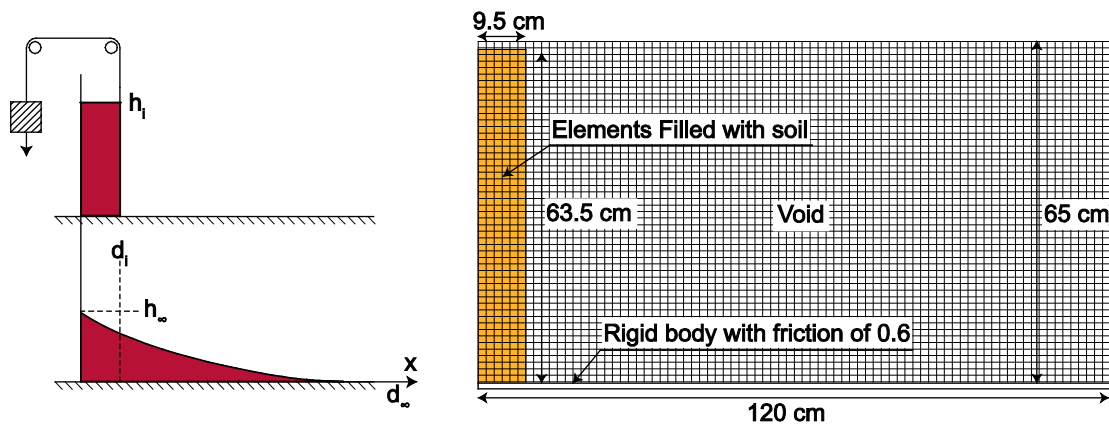


Fig. 6: a) Schematic view of the sand column problem b) initial numerical model configuration

In the numerical model, a 15-mm mesh size is considered. A 3D model with one element in normal direction with plane-strain boundary condition is developed. A void region is defined to let the soil material flow to these elements after the collapse starts. Elements with 1-point integration are used. The gravity acceleration is assigned as 9.806 m/s^2 . The total calculation time of the problem is 2 seconds. The container is modelled as a frictionless rigid body part which is removed as the *In-situ* stresses are initialized. The bottom surface is modelled by a rigid body as well, having a tangential penalty friction equal to soil internal friction angle. The problem is simulated by both Mohr-Coulomb material and the hypoplastic UMAT.

In *Fig. 7*, the final shape of the sand column after collapse is shown. It is observed that an advanced material model in conjunction with an advanced element formulation gives a more realistic behavior. In *Fig. 8*, the run-out distances obtained from Mohr-Coulomb and hypoplastic models are compared with the experimental results. Both the run-out distances and the heights of the sand column predicted by hypoplasticity in different time stamps are closer to the experimental measurements. In addition, the sand column shape during the collapse has a more realistic form compared to the experimental results.

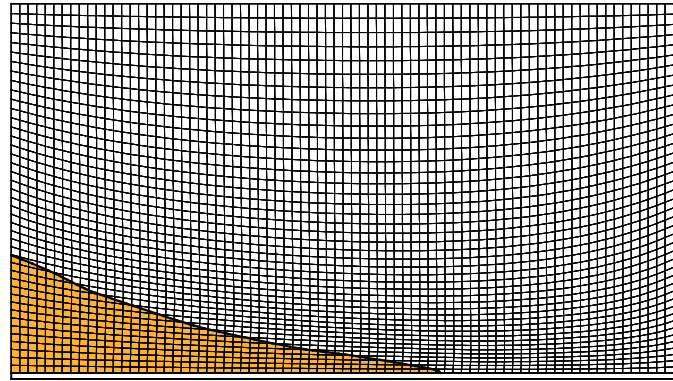


Fig. 7: Final numerical result of the sand shape using the Hypoplastic UMAT

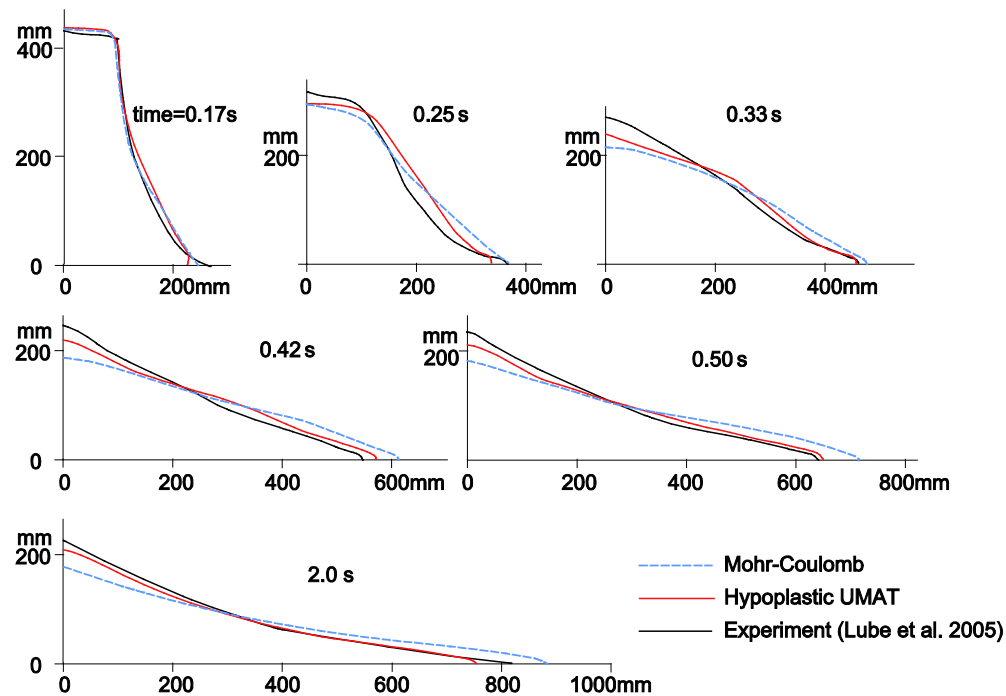


Fig. 8: Comparison of numerical results of sand column shape and distance with experimental measurements

In the UMAT implementation of the hypoplastic model, the void ratio is a history variable which is stored at each time step. In Fig. 9, the void ratio variation is shown after reaching a stable state. By noting the value of 0.695 as the initial void ratio, the left bottom corner compacted due to overburden weight (the green region), while the sliding layers experienced loosening (the red region) as expected. The sudden change in void ratio value at interface region is attributed to the averaged void ratio value for mixed elements of soil and void. Since void ratio of the void elements are zero, the resulting averaged void ratio value becomes smaller than their neighboring elements. Therefore, the values obtained in the interface should be evaluated with care.

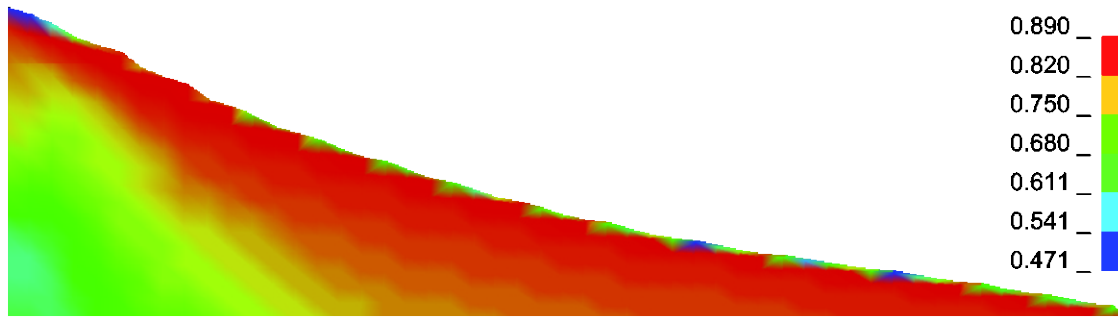


Fig. 9: Void ratio for the Hypoplastic UMAT soil material

Conclusion

LS-DYNA is a powerful finite element code for solving large deformation problems. However, no material model is available in distributed versions that captures complex stress- and density-dependent granular soil behavior for applications in geotechnical engineering. For this purpose, a hypoplastic constitutive model has been implemented. The implementation is done using the user material interface UMAT in LS-DYNA, and tested using several examples of large deformation geotechnical problems. The hypoplastic model implementation was also tested in conjunction with the advanced MMALE element formulation.

The implementation of the UMAT is verified using two principal single-element numerical benchmarks: cyclic oedometer test and cyclic triaxial test. The results obtained are identical to those reported in the literature [10]. Subsequently, a sand column collapse experiment is simulated to evaluate the performance of the hypoplastic model with the advanced MMALE element formulation. By comparing the deformed shape and the run-out distances at several time stations, it was observed that the implemented UMAT performs well in capturing complex soil behavior. By considering the obtained results and its advantages, the implemented Hypoplastic UMAT can be considered as a promising material model for realistic simulations of complex nonlinear soil behavior under large deformations.

References

- [1] Qiu G, Henke S, Grabe J. Application of a Coupled Eulerian-Lagrangian approach on geomechanical problems involving large deformations. *Computers and Geotechnics* 2011;38:30–9. doi:10.1016/j.compgeo.2010.09.002.
- [2] Bakroon M, Aubram D, Rackwitz F. Geotechnical large deformation numerical analysis using implicit and explicit integration. In: Bilsel H, editor. *3rd International Conference on New Advances in Civil Engineering*, Helsinki, Finland: 2017, p. 26–36.
- [3] Pucker T, Grabe J. Numerical simulation of the installation process of full displacement piles. *Computers and Geotechnics* 2012;45:93–106. doi:10.1016/j.compgeo.2012.05.006.
- [4] Dijkstra J, Broere W, Heeres OM. Numerical simulation of pile installation. *Computers and Geotechnics* 2011;38:612–22. doi:10.1016/j.compgeo.2011.04.004.
- [5] Kolymbas D. *Constitutive Modelling of Granular Materials*. Berlin, Heidelberg: Springer Berlin Heidelberg; 2012.
- [6] Kolymbas D. A rate-dependent constitutive equation for soils. *Mechanics Research Communications* 1977;4:367–72. doi:10.1016/0093-6413(77)90056-8.
- [7] Gudehus G. A Comprehensive Constitutive Equation for Granular Materials. *Journal of the Japanese Geotechnical Society : Soils and Foundation* 1996;36:1–12. doi:10.3208/sandf.47.887.
- [8] Bauer E. Calibration of a comprehensive constitutive equation for granular material. *Soils and Foundations* 1996;36:13–26.
- [9] von Wolffersdorff P. A hypoplastic relation for granular materials with a predefined limit state surface. *Mechanics of Cohesive-Frictional Materials* 1996;1:251–71.
- [10] Niemunis A, Herle I. Hypoplastic model for cohesionless soils with elastic strain range. *Mechanics of Cohesive-Frictional Materials* 1997;2:279–99.
- [11] Gudehus G, Amorosi A, Gens A, Herle I, Kolymbas D, Mašin D, et al. The soilmodels.info project. *International Journal for Numerical and Analytical Methods in Geomechanics* 2008;32:1571–2. doi:10.1002/nag.675.
- [12] Hirt CW, Amsden AA, Cook JL. An Arbitrary Lagrangian-Eulerian Computing Method for All Flow Speeds. *Journal of Computational Physics* 1974;14:227–53.
- [13] Bakroon M, Daryaei R, Aubram D, Rackwitz F. Arbitrary Lagrangian-Eulerian Finite Element Formulations Applied to Geotechnical Problems. In: Grabe J, editor. *Numerical Methods in Geotechnics*, Hamburg, Germany: Elbe-Werkstätten GmbH; 2017, p. 33–44. doi:978-3-936310-43-6.
- [14] Benson DJ. Computational methods in Lagrangian and Eulerian hydrocodes. *Computer Methods in Applied Mechanics and Engineering* 1992;99:235–394. doi:10.1016/0045-7825(92)90042-I.
- [15] Aubram D, Rackwitz F, Savidis SA. Contribution to the non-lagrangian formulation of geotechnical and geomechanical processes. *Lecture Notes in Applied and Computational Mechanics*, vol. 82, Springer International Publishing; 2017, p. 53–100. doi:10.1007/978-3-319-52590-7_3.
- [16] Reyes DK, Rodriguez-Marek A, Lizcano A. A hypoplastic model for site response analysis. *Soil Dynamics and Earthquake Engineering* 2009;29:173–84. doi:10.1016/j.soildyn.2008.01.003.
- [17] Herle I, Gudehus G. Determination of parameters of a hypoplastic constitutive model from properties of grain assemblies. *Mechanics of Cohesive-Frictional Materials* 1999;4:461–86. doi:10.1002/(SICI)1099-1484(199909).
- [18] Lube G, Huppert HE, Sparks RSJ, Freundt A. Collapses of two-dimensional granular columns. *Physical Review E - Statistical, Nonlinear, and Soft Matter Physics* 2005;72:41301. doi:10.1103/PhysRevE.72.041301.
- [19] Solowski WT, Sloan SW. Modelling of sand column collapse with material point method. In: Gyan Pande SP, editor. *Proceeding of the Third International Symposium on Computational Geomechanics (ComGeo III)*, vol. 553, Krakow, Poland: 2013, p. 698–705.